

ON THE CRACK STABILITY IN METAL PARTICULATE - REINFORCED BRITTLE MATRIX COMPOSITES

M. Kotoul¹ and R. Urbíš¹

¹Department of Solid Mechanics, Brno University of Technology, Technická 2,
616 69 Brno, Czech Republic

ABSTRACT

The model of reinforcing mechanism which improves the fracture toughness of brittle matrix composites reinforced by ductile particles is analyzed. The particles form a bridging zone and, thus, constrain the crack opening. The stress-crack opening displacement relationship relies upon the constant volume plastic flow of the particles according to the model suggested recently by Rubinstein and Wang [1]. This model incorporates in a certain way also the particle/matrix interface properties. The particles are allowed to deform using several different patterns which correspond to the particular strength of the particle/matrix interface. Contrary to Rubinstein and Wang's work the triaxiality of the stress state within particles is considered and its impact on the critical crack opening displacement is included. The fracture criteria are analyzed for several combinations of micromechanical parameters of composite system and the resistance curves are presented.

KEYWORDS

Fracture toughness, particulate composites, bridged cracks.

INTRODUCTION

In certain materials, the opening of a crack may be opposed by physical bridges between the crack faces. One example is a ceramic containing ductile metal particles (a particulate-reinforced ceramic). The restraining effect of the second-phase particles on an advancing crack front is the basis for a toughness increment. Stretched ductile particles (ligaments), e.g. Al particles in Al₂O₃/Al systems or Co enclaves in WC/Co composites, are detected at considerable distances l_p behind the crack tip. The basics of the mechanism of fracture toughness enhancement in brittle matrix composites with distributed ductile particles were analyzed in the literature, e.g. [3-6].

It is important to note that the particles's ductility alone is not sufficient for any significant improvement in toughness. It is observed that the quality of the particle/matrix interface also becomes of great importance because it strongly influences the particle deformation pattern. Specifically, some optimum interface debonding is needed to remove the geometric constraint and allow the particles to deform plastically in a significant part of their volume. An analytical approach, allowing detailed calculation of the development of the fracture toughness during loading, was presented by Rubinstein and Wang [1]. Particles were assumed to be elastic-ideally plastic and allowed to deform using several different patterns which correspond to the particular strength of the particle/matrix interface. The deformation patterns were simplified versions of those obtained by Tvergaard [2] using finite element computations. Namely, the initially spherical particles of the same radius R simultaneously

form during the plastic deformation a neck of a parabolic profile, as illustrated in Figure 1. The current radius of the bridging cross section of a particle r , the vertical coordinate of the intersection of the parabolic neck with the undisturbed spherical portion of a particle y_{pn} and the half of the crack opening displacement at the particle site $\Delta/2$ within the bridging zone are then related by

$$\frac{r}{R} = \sqrt{1 - \left(\frac{y_{pn}}{R} - \frac{\Delta}{2R}\right)^2} - A \left(\frac{y_{pn}}{R}\right)^2, \quad (1)$$

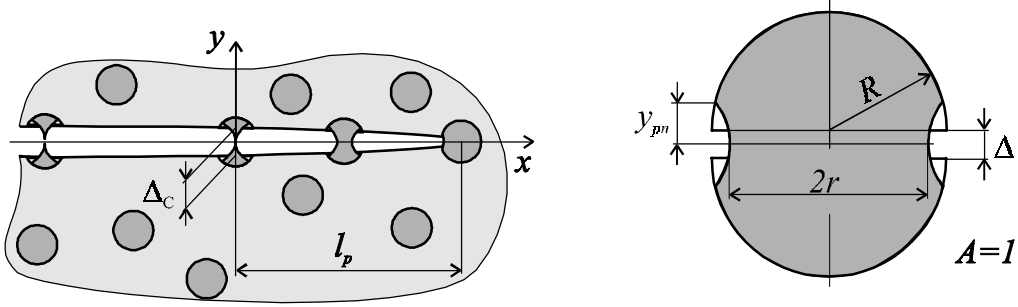


Figure 1: Scheme of bridged crack and particle deformation shape for $A = 1$

where parameter A specifies the curvature of the chosen parabolic profile, $x'/R = A(y/R)^2 + r/R$. The authors [1] suggest to associate this parameter with the strength of the particle/matrix interface and to use it as a parameter of the composite. The requirement of incompressibility of the particles provides then the additional condition for determination of r , y_{pn} and $\Delta/2$:

$$2 = \left(1 - \frac{y_{pn}}{R} + \frac{\Delta}{2R}\right)^2 \left(2 + \frac{y_{pn}}{R} - \frac{\Delta}{2R}\right) + 3 \left[\frac{1}{5} A \left(\frac{y_{pn}}{R}\right)^2 + \frac{2}{3} A \frac{r}{R} \left(\frac{y_{pn}}{R}\right)^3 + \frac{y_{pn}}{R} \left(\frac{r}{R}\right)^2 \right]. \quad (2)$$

A significant simplification was introduced in [1] by assuming a constant stress within the bridging section of each particle. In this paper we will make use of Eqns. 1. and 2. for analytical modelling of debonding of particle/matrix interface. The mean axial stress in the necked bridging section of particles is, however, assumed not to be constant but given by Bridgman's solution. The action of the system of discretely distributed ideally plastic particles is replaced by the action of smeared forces over the bridged zone length l_p . Small scale bridging is assumed, i.e. $l_p \ll a$, where a is the crack length. Thus, a semi-infinite crack, $x < 0$, $y = 0$, may be considered. The remote load is given through the boundary layer approach, so that the stress $\sigma_{yy} = K_I^N / \sqrt{2\pi x}$ for $x \gg l_p$, $y = 0$, where K_I^N is the remote stress intensity factor which can be found by solving an appropriate boundary value problem on the macrolevel using e.g. FEM.

MATHEMATICAL MODELLING

The continuously distributed crack surface bridging load σ_0 can be determined as follows: if R is the average particle radius, l is the interparticle distance and f is the volume fraction of particles, then the restraining stress σ_0 is found to be $\sigma_0 = P/l^2 = P/R^2 (3f/4\pi)^{2/3}$, where P is the bridging force of a single particle. The bridging force P relates to the mean axial stress σ_1 in the necked region of a particle and to the current radius of the bridging cross section of a particle r as $P = \pi r^2 \sigma_1$. The mean axial stress σ_1 is estimated from Bridgman's solution:

$$\sigma_1 = \sigma_y \left(1 + \frac{R}{Ar}\right) \ln \left(1 + \frac{Ar}{R}\right), \quad (3)$$

where $1/(2A)$ is the radius of curvature of the necked region profile in the normalized coordinates x'/R and y/R , see above, and σ_y is the uniaxial yielding stress of the ductile particle. Finally, the restraining stress σ_0 can be estimated as

$$\sigma_0 = \sigma_y \left(\frac{3f\sqrt{\pi}}{4}\right)^{2/3} \left(\frac{r}{R}\right)^2 \left(1 + \frac{R}{Ar}\right) \ln \left(1 + \frac{Ar}{R}\right). \quad (4)$$

In order to obtain the restraining stress σ_0 as a function of the normalized crack opening displacement Δ/R within the bridging zone for the specified curvature of the chosen parabolic profile of the particle's neck, the normalized vertical coordinate y_{pn}/R of the intersection of the parabolic neck with the undisturbed spherical

portion of a particle is first eliminated between Eqns. 1. and 2. and the normalized current radius of the bridging cross section r/R is expressed as a function of Δ/R . Figure 2 shows the plots of the bridging cross

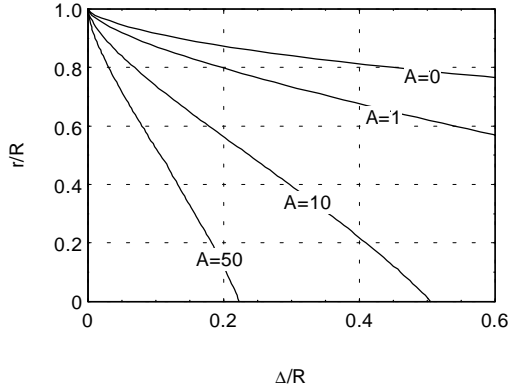


Figure 2: Plots of the bridging cross section r/R vs. Δ/R for several values of A

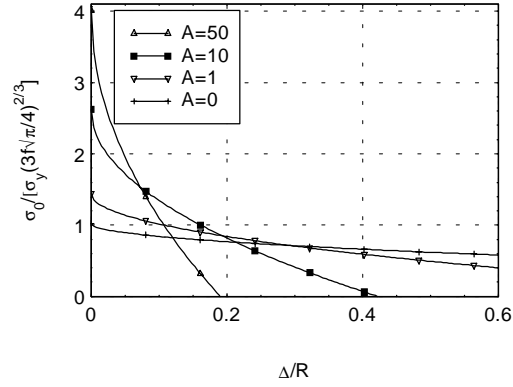


Figure 3: Plots of the normalized restraining stress vs. Δ/R for several values of A

section r/R against $\Delta/2R$ for several values of A . If the relation $r/R - \Delta/R$ is substituted into Eqn. 4. a desired function $\sigma_0(\Delta/R)$ is obtained. Figure 3 shows the course of the normalized restraining stress $\sigma_0 / \left[\sigma_y \left(\frac{3f\sqrt{\pi}}{4} \right)^{2/3} \right]$ vs. the normalized half crack opening displacement $\Delta/2R$ for several values of the parameter A for ideally plastic material. Plots in Figure 3 indicate that the slope of $\sigma_0(\Delta/R)$ curve is negative in the stage of the plastic deformation of bridging particles and the bridging zone here exhibits softening behaviour. For the purpose of further analysis there is convenient to have a simple mathematical approximation of the curves in Figure 3. These curves were fitted to the function linear in $\sqrt{\Delta/R}$, i.e.

$$\frac{\sigma_0}{\sigma_y \left(\frac{3f\sqrt{\pi}}{4} \right)^{2/3}} \doteq -a\sqrt{\frac{\Delta}{R}} + b, \quad (a > 0, b > 0). \quad (5)$$

Individual fits are not shown in Figure 3 because they are barely distinguishable from the exact numerical curves. The square root dependence of the normalized restraining stress upon the crack opening displacement in Eqn. 5. allows to use a simple perturbation method to the solution of the resulting integral equation.

The analytical formulation is based on the distribution dislocation technique and the boundary layer approach through which the remote load is introduced. The dislocation distribution is introduced only along the bridging zone, the traction-free crack faces are modelled via mirror stresses. The equilibrium condition across the bridging zone leads to a singular integral equation for the unknown Burgers vector density $b_y(x) = -\frac{d\Delta(x')}{dx'}$. Normalizing the integration interval to $(-1, 1)$ and integrating by part we obtain after some algebra a strongly singular integral equation for the unknown normalized crack opening displacement $\Delta(\rho')/R$ as follows

$$\oint_{-1}^1 \frac{d\rho'}{(\rho' - \rho)^2} \frac{\Delta(\rho')}{R} + \int_{-1}^1 \frac{d\rho'}{(\rho' + \rho + 2)^2} \frac{\Delta(\rho')}{R} = -\frac{2(1 - \nu^2)}{ER} \left[\sqrt{2\pi} \sqrt{l_p} K_I^N - \pi(\rho + 1) l_p \sigma_0 \left(\frac{\Delta}{R} \right) \right], \quad (6)$$

where E is the Young modulus of and ν Poisson's ratio of composite, the symbol \oint_{-1}^1 denotes the finite part of the improper (strongly singular) integral in the sense of Hadamard.

NUMERICAL SOLUTION

Substitute the fit of the restraining stress σ_0 from Eqn. 5. in Eqn. 6. and rewrite it formally as

$$L_{-1}^1 \left[\frac{\Delta}{R} \right] (\rho) + \varepsilon \Lambda(\rho) \sqrt{\frac{\Delta(\rho)}{R}} = \Psi(\rho), \quad (7)$$

where L_{-1}^1 is the integral operator defined by Eqn. 6, $\Lambda(\rho)$ and $\Psi(\rho)$ are linear functions $\Lambda(\rho) = a(\rho + 1)$, $\Psi(\rho) = \varepsilon b(\rho + 1) - \kappa$, where $\kappa = \frac{2(1-\nu^2)}{E} \sqrt{2\pi} \frac{\sqrt{l_p}}{R} K_I^N$ and ε is a parameter defined by

$$\varepsilon = \frac{2\pi(1-\nu^2)}{E} \sigma_y \left(\frac{3f\sqrt{\pi}}{4} \right)^{2/3} \frac{l_p}{R}, \quad (8)$$

which, in a wide range of typical values of materials properties, fulfills the inequality $\varepsilon < 1$. For $\varepsilon < 1$ an asymptotic expansion of $\Delta(\rho)/R$ in terms of ε can be considered

$$\frac{\Delta(\rho)}{R} \cong \sum_{p=0}^N \varepsilon^p \frac{\phi_p(\rho)}{R}, \quad \phi_p(\rho) = 0 \text{ for } \rho = 1. \quad (9)$$

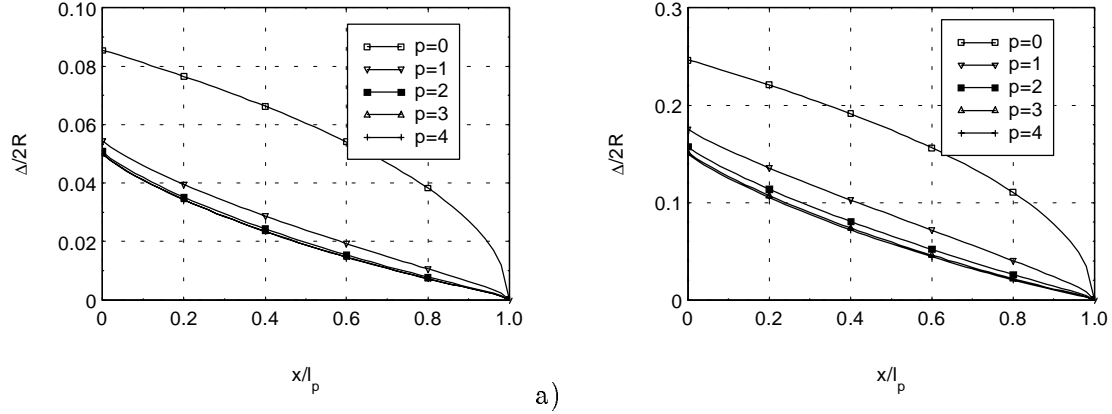


Figure 4: Change of the half of the normalized half crack opening displacement along the bridging zone as the number of terms in (9) increases for $k = 0.5$, $f = 0.25$, $\nu = 0.2$, $A = 1$ and a) $\Delta_c/R = 0.1$, b) $\Delta_c/R = 0.3$.

After substituting Eqn. 9 into Eqn. 7, a system of recursive linear singular equations for the coefficients of the corresponding powers of the parameter ε can be obtained. Solutions of these equations may be expressed in the form $\phi_p(\rho) = F_p(\rho) w(\rho)$, where F_p is unknown bounded function and $w(\rho) = \sqrt{1-\rho}$. The unknown function F_p is approximated by a truncated series as $F_p(\rho) \cong \sum_{j=0}^s a_{pj} \rho^j$ and the coefficients a_{pj} are determined by a simple collocation method. The influence of the number of terms in the asymptotic expansion of $\Delta(\rho)/R$ in Eqn. 9, is illustrated in Figure 4 which shows a change of the crack opening displacement along the bridging zone as the number of terms in Eqn. 9 increases for specified values of composite parameters and two values of Δ_c/R . The ratio of σ_y/E is not expected to vary significantly for different composite systems and is set to a reasonable value of 0.001. Once the solution is obtained, the local stress intensity K_I^{loc} is determined using the standard formula, see e.g. [7]:

$$K_I^{loc} = \frac{E}{2(1-\nu^2)} \lim_{\rho \rightarrow 1^-} \frac{\sqrt{\pi} \Delta(\rho)}{\sqrt{2l_p(1-\rho)(\rho+3)}} = \frac{K_{IC}}{8(1-\nu^2)} \frac{E}{\sigma_y} \frac{1}{k} \lim_{\rho \rightarrow 1^-} \frac{\pi \frac{\Delta(\rho)}{R}}{\sqrt{\frac{l_p}{R}(1-\rho)(\rho+3)}}, \quad (10)$$

where K_{IC} is the fracture toughness of the matrix and $k = \frac{K_{IC}}{2\sigma_y} \sqrt{\frac{\pi}{2R}}$ is another composite parameter which combines the fracture toughness of the matrix with the yield strength and the radius of the particles. Crack growth in the matrix is controlled by the value of the local stress intensity factor; it has to reach the critical value for the matrix K_{IC} . The bridged zone length l_p is controlled by the crack opening displacement which has to reach a critical value Δ_c . Thus, the fracture criteria are as follows

$$K_I^{loc} = K_{IC}, \quad \Delta = \Delta_c. \quad (11)$$

NUMERICAL RESULTS AND DISCUSSION

Equations 11, have been solved for unknowns K_I^N/K_{IC} and l_p/R with various combinations of the parameters A , k , Δ_c/R , f , σ_y/E and ν . A solution for K_I^N/K_{IC} is denoted by $(K_I^N/K_{IC})_{eff}$. This value, which is called the normalized effective fracture toughness of composite, describes the toughening effect of ductile particles.

The following computational strategy is adopted; for a given value of the parameter A the unknowns K_I^N/K_{IC} and l_p/R are calculated as functions of the normalized critical crack opening displacement Δ_c/R on a interval

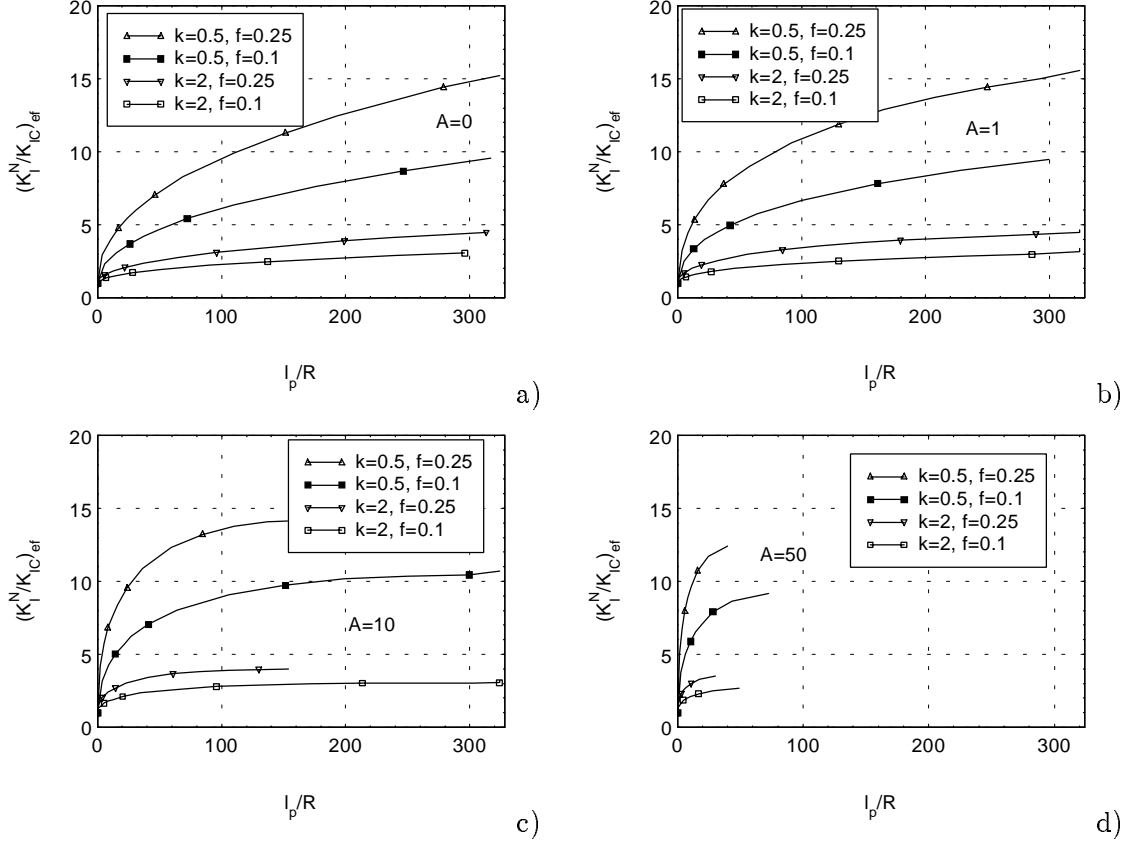


Figure 5: Plots of the normalized effective fracture toughness $(K_I^N/K_{IC})_{eff}$ vs. the normalized length of the bridged zone l_p/R for two different values of the volume fraction f and the parameter k and a) $A = 0$, b) $A = 1$, c) $A = 10$, d) $A = 50$.

$0 < \Delta_c/R \leq \Delta_{max}/R$, where Δ_{max}/R is the intercept of the $\sigma_0 - \Delta/R$ relation with the Δ/R axis, see Figure 3. These calculations are performed for several values of the volume fraction of particles f and the composite parameter k . Thus, for each value of Δ_c/R (with f and k held constant) a pair of values of $(K_I^N/K_{IC})_{eff}$ and l_p/R is obtained which allows to plot $(K_I^N/K_{IC})_{eff}$ against l_p/R by changing Δ_c/R . The plots are shown in Figure 5. Note that with f held constant a higher value of the composite fracture resistance is predicted with decreasing value of the parameter k , i.e. with increasing the size of particles in a specified material system. The same trend was predicted in [1]. So far Δ_c/R has been treated as an independent model parameter and has changed arbitrarily within the interval $(0, \Delta_{max}/R)$. Note that Δ_c/R depends on the particle ductility and the stress triaxiality as well. The latter is governed by the parameter A which specifies the curvature of the chosen parabolic profile and associates with the strength of the particle/matrix interface. To compare an increase in the toughness $(K_I^N/K_{IC})_{eff}$ for different A , the stress triaxiality factor should be included. To do this, a rupture criterion of bridging particles has to be formulated. Widely used in the local approach of ductile fracture is the criterion based on the Rice and Tracey [8] equation for the growth of an initially spherical void. On integrating this equation with the assumption that stress state remains constant and there is no void nucleation strain, the equivalent fracture strain \bar{e}_{fr} is given by

$$\bar{e}_{fr} \equiv 2 \ln [(R/r)_A]_{fr} = \frac{\ln \frac{\bar{d}_p}{2\bar{p}}}{0.28 \exp\left(\frac{3}{2} \frac{\sigma_m}{\sigma_y}\right)}, \quad (12)$$

where σ_m is the hydrostatic stress, \bar{d}_p and \bar{p} stand for the mean spacing and the mean radius of inhomogeneities respectively. The absolute value of the fracture strain is not matter of interest because we intend only to compare the fracture strains of bridging particles with different curvature of the parabolic neck profile, i.e. with different stress triaxiality factor σ_m/σ_y . Thus, the knowledge of the microstructural parameter $\bar{d}_p/2\bar{p}$ is not essential.

Basing on Eqn. 12. and the relation $r/R = g(\Delta_c/R)$, see Figure 2, a relationship between $(\Delta_c/R)_{A>0}$ and $(\Delta_c/R)_{A=0}$ has been computed for several values of A . Figure 6 indicates that $(\Delta_c/R)_{A>0}$ is significantly reduced for higher values of A comparing to $(\Delta_c/R)_{A=0}$ due to the influence of the stress triaxiality factor.

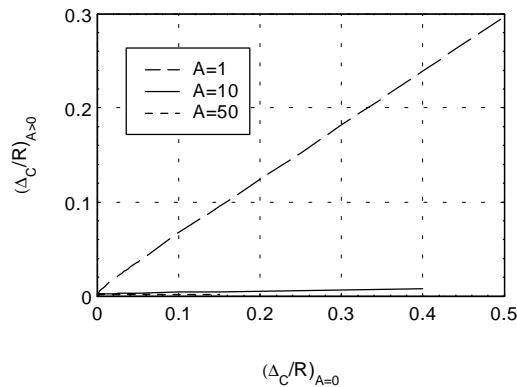


Figure 6: Relation between $(\Delta_c/R)_{A>0}$ and $(\Delta_c/R)_{A=0}$ for several values of A

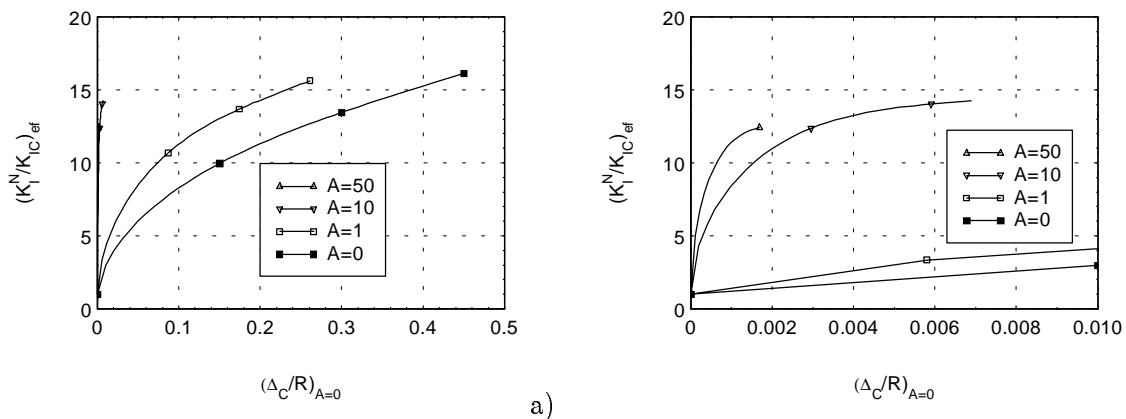


Figure 7: Relation $(K_I^N/K_{IC} |_{A>0})_{eff}$ vs. $(\Delta_c/R)_{A=0}$ including also the effect of the stress triaxiality factor upon the critical crack opening displacement, $k = 0.5$, $f = 0.25$. a) full scale diagram, b) zoomed detail of the left section of the diagram a).

The results in Figure 6 together with the previous computations of $(K_I^N/K_{IC})_{eff}$ provide us with the relation $(K_I^N/K_{IC} |_{A>0})_{eff}$ vs. $(\Delta_c/R)_{A=0}$ as displayed in Figure 7. $(\Delta_c/R)_{A=0}$ serves as an independent variable which characterizes the ductility of bridging particles under the uniaxial stress state condition. Figure 7 reveals two counteracting influences of the particle/matrix interface strength. E.g., the cases of weak interface, i.e. low values of A , allow for higher value of the critical crack opening displacement which entails an increase in the fracture resistance of composite; however, due to the low stress triaxiality in this case, the restraining stress σ_0 is rather low, see Figure 3 and, consequently, the restraining stress intensity factor is also low which reduces the fracture resistance of composite. Summarizing, a certain optimal interfacial debonding is required to achieve an optimal fracture toughness of composite. At the same time, Figure 7 indicates that the optimal property for the interface is not necessary the case of $A = 0$ as stated elsewhere [1].

Acknowledgments-The support through grant GAČR No. 101/99/0829 and the Research Project No. MSM 262100001 is gratefully acknowledged.

1. Rubinstein, A.A. and Wang, P. (1998) *J. Mech. Phys. Solids* 46, 1139.
2. Tvergaard, V. (1992) *Int. J. Mech. Sci.* 34, 635.
3. Rose, L.R.F. (1987) *J. Mech. Phys. Solids* 35, 383.
4. Budiansky, B., Amazigo, J. and Evans, A.G. (1987) *J. Mech. Phys. Solids* 36, 167.
5. Erdogan, F. and Joseph, P.F. (1989) *J. Am. Ceram. Soc.* 72, 262.
6. Bao, G. and Hui, C-Y. (1990) *Int. J. Solids Structures* 26, 631.
7. Kotoul, M. and Urbš, R. (2000) *Eng. Frac. Mechanics* 68, 89.
8. Rice, J.R. and Tracey, D.M. (1969) *J. Mech. Phys. Solids* 17, 201.